



Universidade do Estado do Rio de Janeiro

Centro de Tecnologia e Ciências

Faculdade de Engenharia

Alcéstes Guanabarro de Oliveira Filho

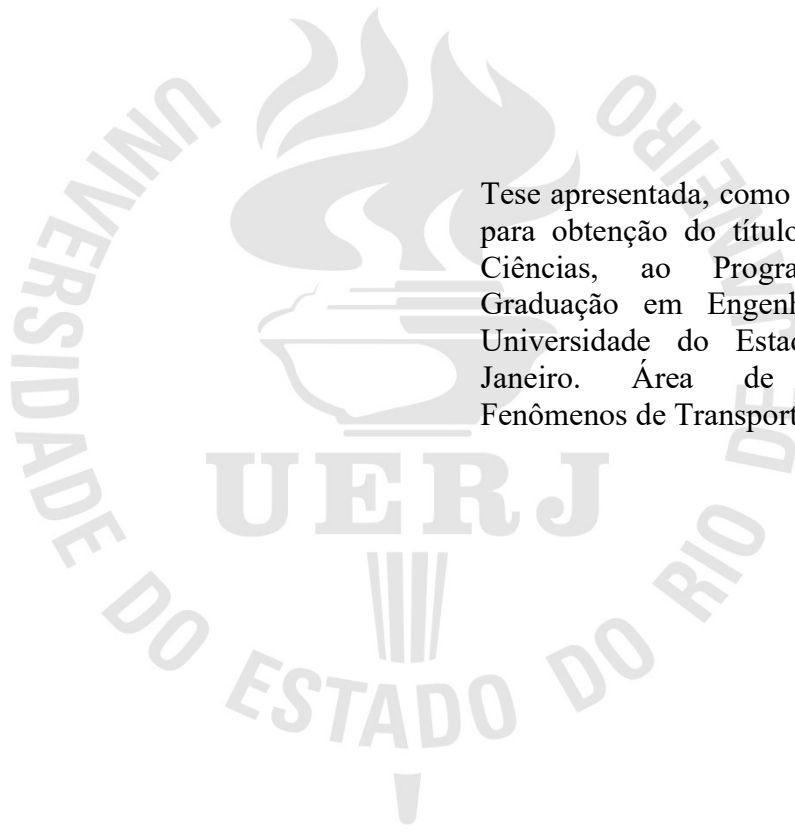
**Two-dimensional reactive flow simulation through a vorticity-stream
function formulation with buoyant term using finite elements method**

Rio de Janeiro

2017

Alcésstes Guanabarro de Oliveira Filho

**Two-dimensional reactive flow simulation through a vorticity-stream function
formulation with buoyant term using finite elements method**



Tese apresentada, como requisito parcial para obtenção do título de Doutor em Ciências, ao Programa de Pós-Graduação em Engenharia Mecânica, Universidade do Estado do Rio de Janeiro. Área de Concentração: Fenômenos de Transporte.

Advisor: Prof. Ph.D. Noberto Mangiavacchi

Assitant Advisor: Prof. D. Sc. José Pontes

Rio de Janeiro

2017

CATALOGAÇÃO NA FONTE
UERJ / REDE SIRIUS / BIBLIOTECA CTC/B

O48 Oliveira Filho, Alcésstes Guanabarino de.
Two-dimensional reactive flow simulation through a vorticity-stream function formulation with buoyant term using finite elements method / Alcésstes Guanabarino de Oliveira Filho. – 2017.
139f.

Orientador: Norberto Mangiavacchi.
Coorientador: José Pontes.
Tese (Doutorado) – Universidade do Estado do Rio de Janeiro, Faculdade de Engenharia.

1. Engenharia Mecânica - Teses. 2. Escoamento - Teses. 3. Teoria do transporte - Teses. 4. Mecânica dos fluidos - Teses. 5. Método dos elementos finitos - Teses. I. Mangiavacchi, Norberto. II. Pontes, José. III. Universidade do Estado do Rio de Janeiro. IV. Título.

CDU 538.95

Bibliotecária: Júlia Vieira – CRB7/6022

Autorizo, apenas para fins acadêmicos e científicos, a reprodução total ou parcial desta tese, desde que citada a fonte.

Assinatura

Data

Alcéstes Guanabaro de Oliveira Filho

**Two-dimensional reactive flow simulation through a vorticity-stream function
formulation with buoyant term using finite elements method**

Tese apresentada, como requisito parcial para obtenção do título de Doutor em Ciências, ao Programa de Pós-Graduação em Engenharia Mecânica, Universidade do Estado do Rio de Janeiro. Área de Concentração: Fenômenos de Transporte.

Aprovado em: 27 de novembro de 2017.

Banca Examinadora:

Prof. Ph.D. Norberto Mangiavacchi (Orientador)
Faculdade de Engenharia - UERJ

Prof. Dr. José Pontes (Coorientador)
Faculdade de Engenharia – UERJ

Prof. Dr. Daniel José Nahid Mansur Chalhub
Faculdade de Engenharia – UERJ

Prof. Dr. Américo Barbosa da Cunha Júnior
Instituto de Matemática e Estatística - UERJ

Prof. Dr. Itamar Borges Júnior
Instituto de Militar de Engenharia - IME

Prof. Dr. Fernando Pereira Duda
Universidade Federal do Rio de Janeiro – UFRJ
Rio de Janeiro

2017

DEDICATION

I dedicate this thesis to the woman of my life, Luciana, thanking for her unconditional support at all times, especially in the uncertainty, which is very common for those who try to tread new paths. Also, to my daughters, Isabela Maria and Giovana Maria, who understood and forgave the absence of their father in several of their dearest moments. Without you all, no conquest would matter.

ACKNOWLEDGMENTS

The great Albert Einstein taught us that time is relative, but my inability to accelerate near lightspeed prevented time dilation and so, time became the most significant portion of my concerns. Therefore, I would like to start my thanks, yielding my gratitude to the Board of Education of the Mechanical Engineering Program at UERJ who tolerated my slowness.

To my thesis advisor, Prof. Dr. Norberto Mangiavacchi, I thank for his safe guidance, patience and for the opportunity he provided me to work at his side. To his appropriate incentive, I earned all the knowledge that allowed me to carry out this thesis.

To Prof. Dr. José Pontes, my assistant advisor, I thank for his always available exquisite education, for his infinite willingness in revising my texts and for all teachings conveyed.

To Prof. Dr. Rogério Saldanha da Gama, my academic advisor during credits phase, I thank for his commitment, for the quality of his classes and for the unrestricted support.

To Prof. Dr. José Júlio Pedrosa Filho, my gratitude for his invaluable assistance in my preparation to the qualifying exam.

To UERJ, I thank for hosting our work, and to FAPERJ, for supporting part of our research, in spite all the difficulties that are raised to establishments that promote education and research in our country.

I thank to my parents, Noélia and Alcéstes, who, tirelessly, directed me towards the path of the men of good will.

To my wife, Luciana, and my daughters, Isabela Maria and Giovana Maria, whose "joie de vivre" was the balm that relieved me of the heaviest loads, I dedicate my thanks for the support intimately provided to me in every hour.

To my fellow students, my appreciation for their companionship. To Secretaries Sonia Florenzino and Renata Rezende and to Engineer Jorge Martins, my respect for their efforts in providing support services that I needed so much.

My thanks also to Capt. Jakler Nichele Nunes, from the Instituto Militar de Engenharia, for providing remote access to additional computer resources, which became essential to the completion of this work.

Finally, I thank to God, who blessed me with a productive life in which I can still be useful. Thou are my shepherd and I lack nothing.

Try not, do or do not. There is no try.

Master Yoda, In: George Lucas, The Empire Strikes Back

RESUMO

OLIVEIRA FILHO, A. G. de. *Simulação de escoamento reativo bidimensional através de uma formulação função corrente - vorticidade com termo de empuxo, usando o método de elementos finitos*. 2017. 139f. Tese (Doutorado em Engenharia Mecânica) - Faculdade de Engenharia, Universidade do Estado do Rio de Janeiro, Rio de Janeiro, 2017.

A construção de usinas hidrelétricas com a finalidade de suprir a demanda de energia elétrica sempre é apresentada acoplada aos conceitos de aproveitamento de recursos naturais e como sendo mais "limpa" do que a produção termelétrica. Na verdade, essa opção é responsável por grandes impactos ambientais porque a decomposição da matéria orgânica submersa nos enormes reservatórios implica na geração de grandes volumes de gases de efeito estufa. Assim, é interessante estudar formas de modelar este fenômeno. A literatura afirma que tais escoamentos têm características estratificadas, com perfis de densidade e temperatura determinados por ciclos ambientais externos e apresentam dois componentes principais: a velocidade longitudinal, impulsionada pela alimentação e descarga e a velocidade vertical, impulsionada principalmente pela evolução de gás para a superfície. Portanto, foi decidido estudar um modelo de escoamento bidimensional com formulação de função-corrente e vorticidade, levando em conta um perfil de densidade influenciado pelo gás despreendido através da aproximação de Boussinesq. Além disso, tendo em conta a oxidação do metano no reservatório, um termo de caimento é adicionado à equação de transporte da concentração, o que caracteriza um escoamento reativo. Para as simulações, realizadas com o objetivo final de obter perfis de velocidade e concentração, o Método de Elementos Finitos surge como um método viável porque pode manusear equações convectiva-difusivas, cujas condições de contorno são consistentemente integradas na chamada forma fraca do sistema. Tendo em conta os ciclos sazonais característicos dos fenômenos ambientais, soluções analíticas multidimensionais para condições de contorno transientes são propostas. Considerações sobre novas condições de contorno para o transporte da vorticidade, mais ajustadas ao fenômeno do que as usualmente encontradas na bibliografia atual são feitas, o que também é uma inovação. Resultados são obtidos e criticados e dificuldades na implementação do modelo são discutidas. Sugestões para trabalhos futuros também são apresentadas.

Palavras-chave: Escoamentos reativos; Simulação; Formulação de função-corrente e vorticidade; Método de Elementos Finitos.

ABSTRACT

OLIVEIRA FILHO, A. G. de. *Two-dimensional reactive flow simulation through a vorticity-stream function formulation with buoyant term using finite elements method*. 2017. 139f. Tese (Doutorado em Engenharia Mecânica) - Faculdade de Engenharia, Universidade do Estado do Rio de Janeiro, Rio de Janeiro, 2017.

Construction of hydroelectric power plants to supply the demand for electrical energy has always been introduced coupled to the concept of harnessing of natural resources and as being more "clean" than thermoelectric production. Actually, it causes large environmental impacts because decomposition of organic matter submerged in huge reservoirs implies in generation of large volumes of greenhouse gases. Thus, it is of interest to study ways to model this phenomenon. Although reservoir flows comprise mixed water and gases, related literature states that these flows have stratified characteristics with density and temperature profiles determined by external environmental cycles. In these basins, the flow has two main components that draw attention: the longitudinal velocity, driven mainly by feeding inflow and outflow discharge and the vertical velocity, driven mainly by gas evolution to the surface. Therefore, it was decided to study a two-dimensional flow model through stream function vorticity formulation, taking into account the density profile provided by the gas given off through Boussinesq approximation. Also, in view of methane oxidation reaction within the reservoir, a decay term is added to the species transport equation, implying in a reactive flow. For the simulations, with the ultimate goal of obtaining flow velocity and concentration profiles, Finite Elements Method emerges as a viable method which can handle-diffusive convective equations, whose boundary conditions are consistently integrated in the system weak form. In view of the seasonal cycles present in environmental phenomena, multidimensional analytical solutions for transient boundary conditions are proposed. Considerations on novel boundary conditions for the transport of vorticity, more adjusted to the physical phenomena than those currently found in the bibliography are made, which is also an innovation. Results are obtained and criticized and difficulties in the implementation of the model are discussed. Suggestions for further work are also outlined.

Keywords: Reactive flows; Simulation; Vorticity-stream function formulation; Finite Elements Method.

LIST OF FIGURES

Figure 1 – Lake and reservoir view of Itaipu hydroelectric plant	16
Figure 2 – Schematic of stratified flow in reservoirs	17
Figure 3 – Stratified layers illustration.	17
Figure 4 – Gas concentration and temperature in world reservoirs	18
Figure 5 – Characteristic continuous water-column density stratifications as found in lakes and typical layer approximations	19
Figure 6 – Illustration of methane dynamics	19
Figure 7 – Domain shape and surfaces	21
Figure 8 – Problem domain Ω and boundary Γ	22
Figure 9 – 1-D analytical and numerical solutions of equations 29-30	33
Figure 10 – 2-D analytical and numerical solutions of equation 31 (1250 elements mesh FEM; GQ 9 points; Pe=50; time elapsed = 1.20).....	34
Figure 11 – 1-D analytical and numerical solutions with periodic inlet BC (1250 elements mesh FEM; GQ 9 points; Pe=100; time elapsed = 10.0).....	34
Figure 12 – 2-D analytical and numerical solutions with periodic inlet BC	35
Figure 13 – 1-D concentration profile differences – numerical solutions (Outlet BC: 0.5; Outlet NBC: Equation 16; Outlet MDBC: Equation 20).....	36
Figure 14 – Domain surfaces and boundary conditions	41
Figure 15 – Stream function computations for Re = 100	50
Figure 16 – Stream function 1-D plots at arbitrary depth for Re = 100	50
Figure 17 – Stream function, vorticity and longitudinal velocity computation (Re = 100; $\omega_s = 0.0$; outlet EBC; GQ of seven points)	52
Figure 18 – Stream function, vorticity and longitudinal velocity computation (Re = 500; $\omega_s = 0.0$; outlet NBC; GQ of seven points)	52
Figure 19 – Stream function, vorticity and longitudinal velocity computation (Re = 1000; $\omega_s = 0.0$; outlet MDBC; GQ of seven points)	53
Figure 20 – Vertical velocity computations for selected Re and outlet BCs ($\omega_s = 0.0$; GQ of seven points).....	54
Figure 21 – Stream function, vorticity and longitudinal velocity computation (Re = 500; $\omega_s = 1.0$; outlet MDBC; GQ of seven points)	55

Figure 22 – Stream function, vorticity and longitudinal velocity computation (Re =100; $\omega_s = -1.0$; outlet NBC; GQ of seven points)	55
Figure 23 – Stream function, vorticity and longitudinal velocity computation (Re = 100; $\omega_s = 0.0$; outlet MDBC; GQ of seven points)	56
Figure 24 – Stream function, vorticity and longitudinal velocity computation (Re =100; $\omega_s = 1+\cos 2\pi t$; outlet MDBC; GQ of seven points	57
Figure 25 – Stream function, vorticity and longitudinal velocity computation (Re =100; $\omega_s = -(1+\cos 2\pi t)$; outlet MDBC; GQ of seven points)	57
Figure 26 – Stream function, vorticity and longitudinal velocity computation (Re=100; alternate surface vorticity; outlet MDBC; GQ of seven points).	58
Figure 27 – Stream function, vorticity and longitudinal velocity computation (Re = 100; $\omega_s = 0.0$; outlet NBC)	59
Figure 28 – Stream function, vorticity and longitudinal velocity computation (Re = 100; $\omega_s = 1.0$; outlet MDBC)	60
Figure 29 – Stream function, vorticity and longitudinal velocity computation (Re = 100; $\omega_s = - 1.0$; outlet MDBC)	60
Figure 30 – Driven Cavity stream function computations for selected Reynolds numbers	61
Figure 31 – Lid-driven cavity u at $x = 0.5$ and v at $y = 0.5$ for $Re = 10$ and $Re = 100$..	62
Figure 32 – Lid-driven cavity u at $x = 0.5$ and v at $y = 0.5$ for $Re = 400$ and $Re = 1000$	62
Figure 33 – Gas concentration profile computation for different time lapses (Re = 100)	65
Figure 34 – Gas concentration profile for different diffusion coefficients (Re =100; time elapsed = 5.0.)	66
Figure 35 – Gas concentration profile for $k = -2.0$ (Re = 100)	66
Figure 36 – Gas concentration profile for $k = -2.0$ and elapsed time = 20 (Re = 100; $D_x = D_y = 0.5$)	67
Figure 37 – Gas concentration profile for various Re $D_x = D_y = 0.5$; $k = - 1.0$; time elapsed = 10.0)	67
Figure 38 – Gas concentration profile for wind blowing on the reservoir surface ($\omega_s = 1.0$)	68
Figure 39 – Gas concentration profile for wind blowing on the reservoir surface (ω_s	

	= - 1.0)	68
Figure 40 –	Gas concentration profile for cyclic inflow variation (Re = 100)	69
Figure 41 –	Gas concentration profile for cyclic driven surface wind variation (Re = 100)	69
Figure 42 –	Stream function, vorticity and longitudinal velocity (Re = 10; outlet NBC; 1800 triangular elements mesh; GQ of seven points)	79
Figure 43 –	Stream function, vorticity and longitudinal velocity (Re = 10; outlet MDBC; 1800 triangular elements mesh; GQ of seven points)	80
Figure 44 –	Stream function, vorticity and longitudinal velocity (Re = 50; outlet EBC; 900 quadrangular elements mesh; GQ of nine points)	80
Figure 45 –	Stream function, vorticity and longitudinal velocity (Re = 100; outlet MDBC; 900 quadrangular elements mesh; GQ of nine points)	81
Figure 46 –	Stream function, vorticity and longitudinal velocity (Re = 100; outlet EBC; 1800 triangular elements mesh; GQ of seven points)	81
Figure 47 –	Stream function, vorticity and longitudinal velocity (Re = 100; outlet NBC; 1800 triangular elements mesh; GQ of seven points)	82
Figure 48 –	Stream function, vorticity and longitudinal velocity (Re = 500; outlet EBC; 1800 triangular elements mesh; GQ of seven points)	82
Figure 49 –	Stream function, vorticity and longitudinal velocity (Re = 500; outlet NBC; 1800 triangular elements mesh; GQ of seven points)	83
Figure 50 –	Stream function, vorticity and longitudinal velocity (Re = 1000; outlet EBC; 1800 triangular elements mesh; GQ of seven points)	83
Figure 51 –	Stream function, vorticity and longitudinal velocity (Re = 1000; outlet MDBC; 1800 triangular elements mesh; GQ of seven points)	84
Figure 52 –	Vertical velocity computation (Re = 100; 1800 triangular elements mesh; GQ of seven points)	84
Figure 53 –	Vertical velocity computation (Re = 500; 1800 triangular elements mesh; GQ of seven points).....	85

LIST OF TABLES

Table 1 –	Typical composition of biogas	16
Table 2 –	Figure 12 correspondent RMSD	35
Table 3 –	RMSD between 1D analytical and numerical solutions	37
Table 4 –	Prescribed inlet parameters	42
Table 5 –	Imposed outlet parameters	44
Table 6 –	Comparison of literature and obtained stream function and vorticity	62

LIST OF SYMBOLS

ρ	–	Density
ρ_0	–	Density referenced to an initial or standard condition
α	–	Expansion coefficient
T	–	Temperature
T_0	–	Temperature referenced to an initial or standard condition
ω	–	Vorticity
ψ	–	Stream function
μ	–	Viscosity
ν_0	–	Kinematic viscosity referenced to an initial or standard condition
g_y	–	Gravity force vector component in the y coordinate direction
u_i	–	Flow velocity along coordinate x_i
C	–	Species concentration
t	–	Time
x_i	–	Coordinate in an arbitrary direction i
D_x, D_y	–	Averaged diffusion coefficient in the direction of the respective coordinate axis
r	–	Reaction term
Γ	–	Domain control surface
Γ^e	–	Element control surface
Ω	–	Domain shape
Ω^e	–	Element subdomain shape
\bar{u}_i	–	Averaged flow velocity along coordinate x_i
k	–	Chemical reaction decay parameter
C_{inj}	–	Injected averaged concentration
m, n	–	Arbitrary integers 1, 2, 3 ...
w	–	Arbitrary weight function
\bar{u}_x, \bar{u}_y	–	Averaged flow velocity along coordinate x and y , respectively
n_x, n_y	–	Components in x and y coordinates directions of normal vector to surface
\vec{n}	–	Normal vector to domain surface

\bar{e}_x, \bar{e}_y	–	Unitary vectors in x and y coordinates directions, respectively
C_{app}	–	Approximated concentration
NN	–	Number of nodes in the finite element mesh
$S_j(x_i)$	–	Arbitrary shape function
Δt	–	Time step
$\{C_b\}, \{C_{t+1}\}$	–	Concentration vector at arbitrary times t and $t+1$, respectively
$\{B_t\}, \{B_{t+1}\}$	–	Boundary terms vector at arbitrary times t and $t+1$, respectively
$erfc$	–	Complimentary error function
C_o	–	Constant forcing for concentration
Δx_i	–	Element size in the direction of coordinate x_i
Δt_i	–	Time step related to element size Δx_i
Pe	–	Péclet Number
Da	–	Damköhler Number
a_1, a_2	–	Flow profile arbitrary parameters
α	–	Relaxation parameter
$\{\omega_b\}, \{\omega_{t+1}\}$	–	Vorticity vector at arbitrary times t and $t+1$, respectively
$\{F_b\}, \{F_{t+1}\}$	–	Buoyant term vector at arbitrary times t and $t+1$, respectively
γ	–	Parameter defining differencing scheme
ψ_t	–	Stream function related to an arbitrary time t

CONTENTS

	INTRODUCTION.....	16
1	SIMULATION OF SPECIES CONCENTRATION DISTRIBUTION IN REACTIVE FLOWS WITH TIME VARYING BOUNDARY CONDITIONS.....	24
1.1	Outlet Boundary Conditions for the Transport Equation.....	24
1.2	Literature Review.....	24
1.3	Mathematical Formulation.....	25
1.4	Numerical Procedure.....	28
1.5	Analytical Solutions to the CDRE.....	29
1.6	Code, Methods and Verification.....	32
1.7	Use of MDBC compared to EBC and NBC for finite domains.....	36
1.8	Closure.....	37
2	SIMULATION OF 2-D VELOCITY DISTRIBUTION IN A STRATIFIED INCOMPRESSIBLE REACTIVE FLOW WITH BUOYANT TERM.....	39
2.1	Literature Review.....	39
2.2	Mathematical Formulation.....	40
2.2.1	<u>Weak formulation of the transport equations.....</u>	40
2.2.2	<u>Formulation of boundary conditions.....</u>	41
2.2.3	<u>Introduction of the buoyant term.....</u>	45
2.3	Numerical Procedure.....	46
2.3.1	<u>Variables approximation and discretization of the equations.....</u>	46
2.3.2	<u>Computational code scheme.....</u>	48
2.3.3	<u>Sketch of the algorithm.....</u>	48
2.4	Preliminary Tests and Analysis.....	49
2.4.1	<u>Velocity profiles with no wind on the reservoir surface.....</u>	51
2.4.2	<u>Velocity profiles with wind blowing on the reservoir surface.....</u>	54
2.4.3	<u>Cyclic environmental effects simulation.....</u>	56
2.4.4	<u>Velocity profiles simulation with buoyant term.....</u>	58
2.5	Model Verification.....	61

2.6	Closure	63
3	2-D SIMULATION OF GASEOUS SPECIES CONCENTRATION PROFILES IN A HYPOTHETICAL RESERVOIR BASIN WITH REACTIVE STRATIFIED FLOW	64
3.1	Concentration Profile Simulations Tests	64
3.1.1	<u>No wind blowing on reservoir surface</u>	64
3.1.2	<u>Wind blowing on reservoir surface</u>	68
3.1.3	<u>Cyclic environmental effects simulation</u>	69
3.2	Closure	70
	CONCLUSION	71
	REFERENCES	74
	APPENDIX A – Stream Function, Vorticity and Velocity Test Computations without Bouyant Term	79
	APPENDIX B – Matlab Code for Computation of Velocity and Concentration Profiles	86
	APPENDIX C – Lid-Driven Cavity Test Matlab Code	102
	ANNEX A – Paper presented in the XXVI Congresso Nacional de Matemática Aplicada e Computacional (CNMAC)	111
	ANNEX B – Paper to be published in the Brazilian Journal of Chemical Engineering (BJChE)	118

INTRODUCTION

0.1 Preliminaries

Construction of large dams to meet Brazil growing energy needs has always been considered due both to the concept of harnessing natural resources and the fact that fully dominated technology to their deployment is already available in the country. Environmentalists have also reinforced this option as being the most "clean" and safe, although, actually, it may provide environmental impacts even more significant than thermoelectric generation (FEARNSIDE, 2002; St LOUIS et al., 2000).

It is to note that anaerobic decomposition of submerged organic matter in reservoirs implies in generation of large volumes of methane and carbon dioxide that evolve into the atmosphere. A typical composition of this given off gas is presented by Table 1.

Table 1 – Typical composition of biogas

Compound	Formula	%
Methane	CH ₄	50–75
Carbon dioxide	CO ₂	25–50
Nitrogen	N ₂	0–10
Hydrogen	H ₂	0–1
Hydrogen sulphide	H ₂ S	0–3
Oxygen	O ₂	0–0

Source: www.kolumbus.fi, 2007.

As it can be seen, CH₄ and CO₂ are the most important components. Furthermore, it is known that methane is about 21 times more powerful in contributing to global warming than carbon dioxide, maybe the most famous greenhouse gas for the general public. Calculations already performed show that the world 52,000 large dams may contribute with more than four percent of the total warming impact of human activities (ENS, 2007). So, it seems interesting to model this phenomenon, in order to find ways to counteract possible environmental harmful effects in the use of hydroelectric power plants.

0.2 Sketch of Reservoirs Dynamics

Figure 1 – Lake and reservoir view of Itaipu hydroelectric plant



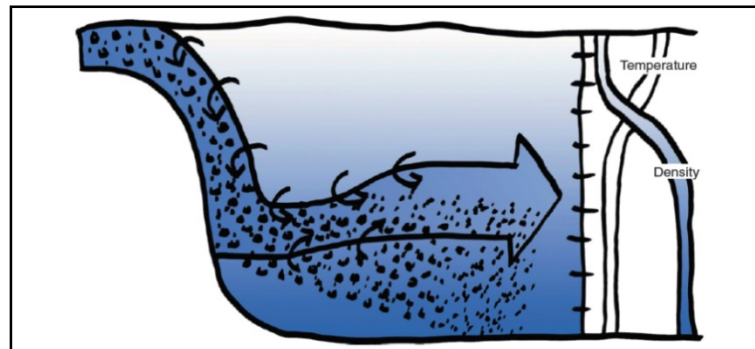
Source: Itaipu Binacional, 2016.

A reservoir is an artificial lake, where flow from a river is impounded by a dam. The flow differs from those of watercourses, like channels and rivers, by the fact that it is far weaker and mostly not driven by gravity but, instead, by surface winds and buoyancy forces (CUSHMAN-ROISIN, 2014).

An also important feature of these water bodies is their great depth which, coupled to weak flow velocities, implies in the consideration of a residence time, defined as the average time spent by a water parcel from time of inflow to that of outflow (CUSHMAN-ROISIN, 2012).

This residence, or retention, time is often large in huge reservoirs and, in this case, the fluid dynamics may be controlled by cyclic variations causing water heating and cooling, affecting its capacity to mix and disperse pollutants (CUSHMAN-ROISIN, 2012). Reservoirs becomes, then, stratified water bodies showing particular flow patterns, as depicted in Figure 2, below, where the shading indicates an increase in density with increasing depth.

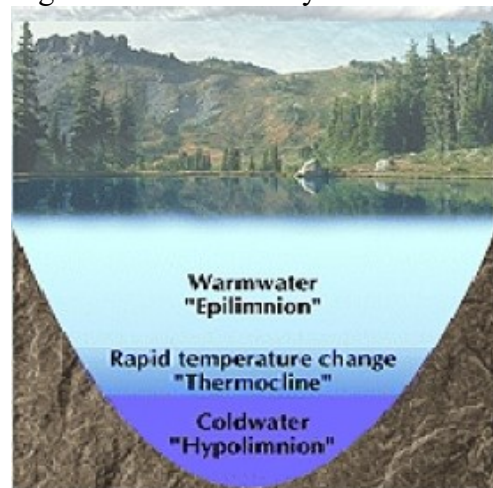
Figure 2 – Schematic of stratified flow in reservoirs



Source: PEETERS; KIPFER, 2009.

Limnology usually defines three layers in such stratified flows (CUSHMAN-ROISIN, 2014):

Figure 3 – Stratified layers illustration



Source: CUSHMAN-ROISIN, 2014.

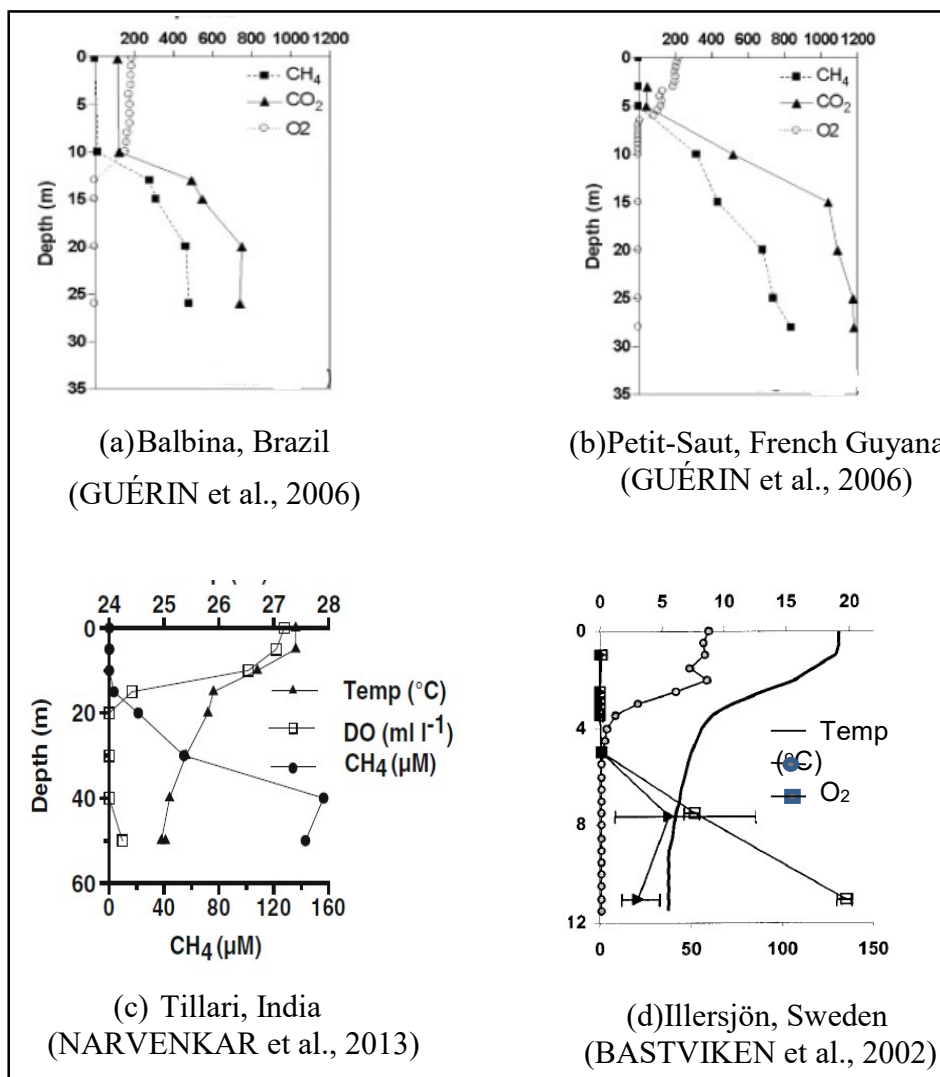
- Epilimnion: affected by surface processes which include wind-driven waves and currents, heating and cooling, aeration, input and discharge of chemical species and pollutants, etc;

- Thermocline: a region of larger vertical temperature and density change;
- Hypolimnion or benthos: affected by the epilimnion and benthic processes such as convection penetrating from above, sedimentation, biological decomposition ensuing oxygen consumption, chemical exchange with bottom sediments, etc.

These layers show proper density profiles caused by temperature, amount of solids in suspension and also by gases concentration that arise from the decomposition of degradable biomass and react with dissolved oxygen to form other products.

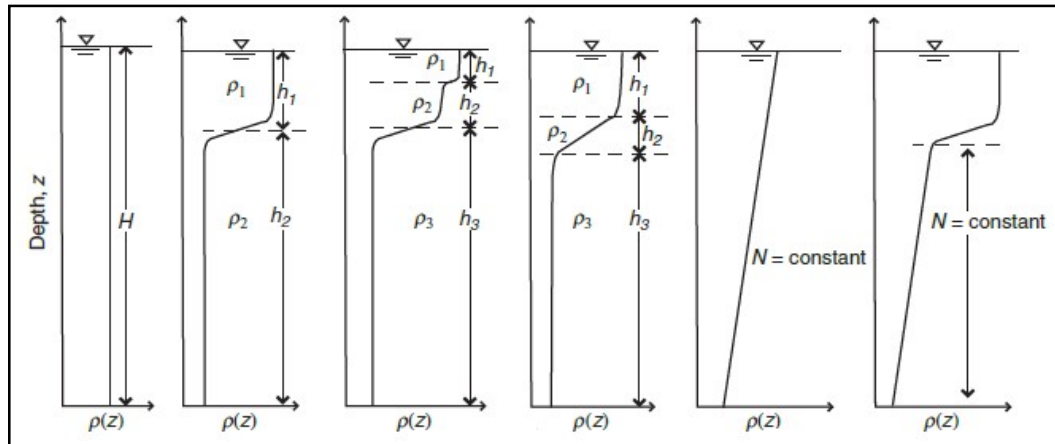
Although quantitatively differing, depending on the reservoir characteristics and location, gas concentration and temperature profiles show similar shapes in its corresponding layers, as illustrated by Figure 4.

Figure 4 – Gas concentration and temperature in world reservoirs



This implies in the generalization of possible density profiles, as proposed by Boegman (2009), illustrated by Figure 5, and makes possible its adoption in a model. It must be remarked also that such vertical density profile, coupled to the longitudinal feature of the reservoir water discharging flow, leads to consideration of a 2-D model, over which this study will be restricted.

Figure 5 - Characteristic continuous water-column density stratifications as found in lakes and typical layer approximations

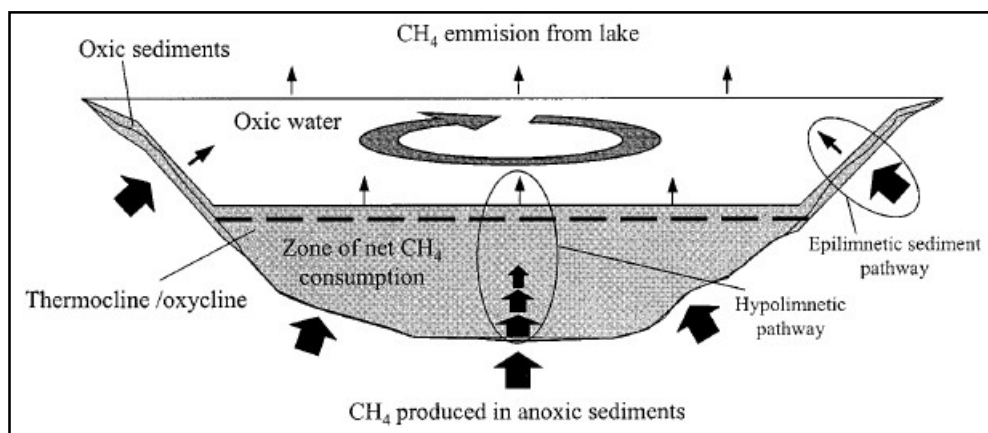


Source: BOEGMAN, 2009.

The first illustration at the left of Figure 5 shows a constant density profile that may be considered for an incompressible but completely mixed flow in only one layer. The second from the left shows constant density profiles in two layers, denoting also complete mixing within the layers, which is also represented by the third illustration, this time, in three layers. The last three figures shows profiles with layers in which the mixing is not uniform and prescribe linear density variations. In any case, the simplicity of these profiles makes possible an implementation in a numerical procedure. Moreover, it may imply that turbulence is restricted to the layers limits, where it is smoothed.

Methane, due to its high proportion in biogas composition and dominance role in global warming, is of major concern. Also, being a known fuel, its use is already being considered for power generation (BAMBACE et al., 2007; LIMA et al., 2008), in addition to hydroelectric generation, which would also have the effect of preventing it of popping out into the atmosphere. So, to complete this sketch, it is worthy the illustration by Bastviken et al. (2002), depicting methane dynamics in stratified reservoirs (Figure 6).

Figure 6 – Illustration of methane dynamics



Source: BASTVIKEN et al., 2002.

Methane is exported from anoxic sediments into the lake where it either accumulates in anoxic bottom waters, gets oxidized in a zone of extensive net methane consumption in

anoxic or oxic water layers and in oxic sediments, or reaches well-mixed surface water and gets emitted to the atmosphere. The zone of net methane consumption indicates where most of the methane is oxidized, although some methane oxidation may occur at lower rates outside that zone.

0.3 Aims and Scope

The objective of the present work is to introduce a formulation that may be applied to a model that simulates the hydrodynamics of hydroelectric power plant reservoirs in presence of greenhouse gases originated from biomass decomposition. It is to expect that computation of this model could afford velocity and concentration profiles that may be used as a basis for the mitigation of harmful effects these gases cause when they are added to the atmosphere. It must also be added that flow dynamics of methane naturally will imply in the study of a reactive flow.

To construct the model, the following considerations are made:

- a) The problem of current interest is the solution of the chemical species transport equation, in order to determine the gas concentration field and, although this implies in the solution of the equations of motion, the velocity field is to be determined rather than to be specified;
- b) The model must incorporate the features of reservoirs dynamics, as sketched above, which imply in the addition of reaction and buoyant terms to the transport equations;
- c) Also, reservoirs are not confined basins, having inflow and outflows currents that need to be modeled;
- d) Water thermal expansion may be described by (CUSHMAN-ROISIN, 2012):

$$\rho = \rho_o [1 - a(T - T_o)] \quad (1)$$

where $a = 2.57 \times 10^{-4}/^{\circ}\text{C}$ and $\rho_o = 999 \text{ kg/m}^3$ for $T_o = 15^{\circ}\text{C}$.

- e) As consequence of Equation 1, even large temperature changes between the surface and the bottom in a reservoir will imply in small density differences. So, it is possible to consider incompressibility of the flow within the layers and the vorticity-stream function formulation is employed;
- f) In order to reduce computational cost in the resolution of the governing equations, the energy equation will not be considered, by assuming that density variations are coupled to thermal changes in the waterbed. In fact, in such environments, the energy equation may be assumed decoupled from the continuity and further governing equations, because the temperature profiles are induced from external weather conditions;
- g) Due to the usual large dimensions of reservoirs and to velocity and concentration components, multidimensional formulations are necessary;
- h) Reservoirs weak flow velocities point at the analysis of flows only at moderate Reynolds Numbers and so, averaged hydrodynamic fields will be assumed without the introduction of turbulence models in the evolution equations.

In view of these considerations, the problem will be addressed by:

- a) 2-D Navier-Stokes equations in the stream-function formulation, incorporating a buoyant term originated through the Boussinesq approximation, which is obtained as described by Aziz and Hellums (1967):

$$\frac{\partial \omega}{\partial t} + \text{rot} \psi \cdot \nabla \omega = \nu_o \nabla^2 \omega - \frac{\partial \rho^*}{\partial x} g_y \quad (2)$$

$$\nabla^2 \psi = -\omega \quad (3)$$

$$\text{where: } \omega = \frac{\partial u_y}{\partial x} - \frac{\partial u_x}{\partial y}, \quad u_x = \frac{\partial \psi}{\partial y}, \quad u_y = -\frac{\partial \psi}{\partial x} \quad \text{and} \quad \rho^* = \frac{\rho}{\rho_o}.$$

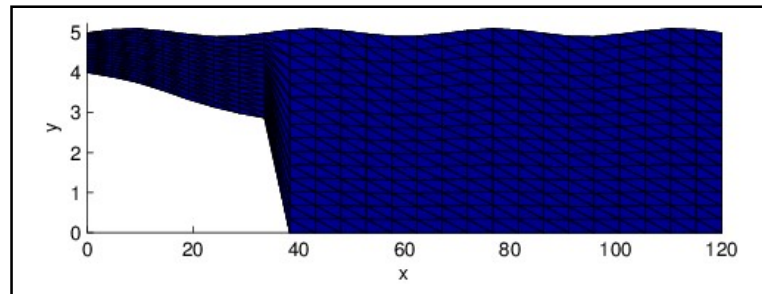
- b) 2-D Convection-Diffusion-Reaction Equation (CDRE) for the gas concentration (C):

$$\frac{\partial C}{\partial t} = -\vec{u} \cdot \nabla C + \nabla \cdot [\overline{\overline{D}} \nabla C] - r \quad (4)$$

- c) where, for 2-D flows, the diffusion coefficient is defined as $\overline{\overline{D}} = \begin{bmatrix} D_x & 0 \\ 0 & D_y \end{bmatrix}$ and r is the decay term related to the gas.

- d) It must be observed, however that, in the proposed vorticity-stream function formulation, the velocity vector in Equation 4 is associated to the stream function as mentioned in item “a” above;
- e) Domain shape and surfaces representing a reservoir basin with inflow by the left boundary and the right boundary representing the dam and outflow surface. A possibility is illustrated by the following figure.

Figure 7 – Domain shape and surfaces.



0.4 Numerical Procedure and Code Programming

The numerical procedure will be approached by the Finite Elements Method (FEM), which is a viable alternative, showing necessary flexibility to deal with problems of multidimensional reactive flows in complex geometries and to reach the expected results. The FEM formulation used is known as Galerkin FEM (GFEM), in which weight functions are selected as the shape functions, or, for 2-D: $w(x, y) = S_i(x, y)$.

For some time, FEM has been employed in the study of fluid flows of various characteristics and its use, based on weighted residues approach with a Galerkin formulation. A fundamental reference for time-dependent Navier-Stokes equations approximation is Taylor

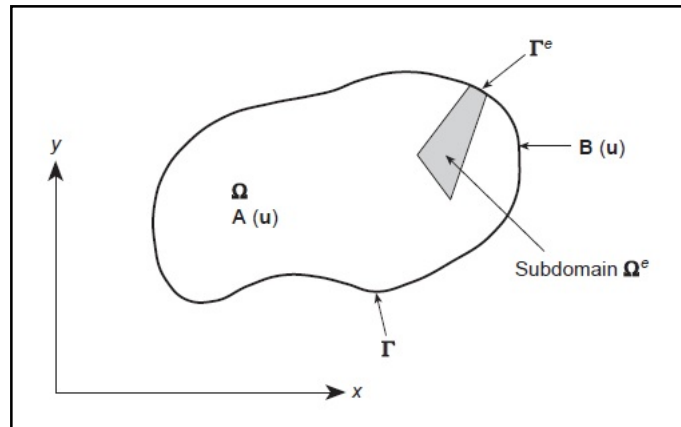
and Hood (1973) and, for reactive flows, Finlayson (1972, 1980), whose developments need to be widened and adjusted to the case in view.

Gauss Quadrature (GQ) appears as one of the most preferred integration technique to be used in FEM (SERT, 2015). By this technique, integrals are evaluated between special unitary limits, implying in the concept of using master element. The original element form is not lost, however, because it is possible to perform proper coordinate changes through Jacobian transformations, which need to be programmed.

A major contribution is also expected to be achieved with a new form of defining boundary conditions (BCs) for the transport equations. As many other continuum problems that arise in engineering and physics, the one under study is posed by appropriate differential equations, already referred, whose BCs, applied to the unknown functions that solve the problem, individualize a depicted situation.

As it is illustrated by Figure 8, we seek a function \mathbf{u} such that it satisfies a certain differential equation set \mathbf{A} in the domain Ω , subjected to restrictions at the boundaries Γ ($\mathbf{B}(\mathbf{u})$).

Figure 8 – Problem domain Ω and boundary Γ



Source: ZIENKIEWICZ; TAYLOR, 2000.

If the BCs are known, probably supplied by experimental measures, they must be imposed at the boundaries, necessarily forcing the observed values. But in the case of simulations occurring prior to experimental activity, these boundaries need to be predicted. It must be observed that these BC may be difficult to predict, mainly in the case of time dependent inputs, as is the case of flows occurring under environmental variations. It seems then that the best way of doing this is to extend the physics of the problem, described by the differential equations, to the boundaries. This is attempted by introducing a new form of BC, as is addressed in the following sections.

In order to make programming an easier task, an option was made towards adoption of MATLAB language, where built-in routines provide numerous resources to treat matrix and vector calculations. However, it must be remarked that although MATLAB can perform symbolic integration, the integrals in the formulation are evaluated numerically, in a more flexible and much faster way. By doing so, a code that is easier to translate into a lower level language is also made available.

As a matter of fact, programming in a language that would allow faster computation is, naturally, one of the next steps of this work. So, the aim of elaborate the code by writing its routines with minimum use of MATLAB private resources is pursued.

0.5 Model Verification and Implementation

Simulations are very useful not only when they reproduce previously obtained experimental data, but also when they are able to anticipate results. Whatever is its purpose, the model has to be verified and the comparison between numerical and analytical solutions is one way to attain it.

Thus, the verification is pursued in two steps:

1) Compare results from the species transport equation for the gas transport with predefined flow velocity profile to analytical solutions. It is to note that most classical solutions of the species transport equation often restrict their analysis to one-dimensional spaces, while the model demands bi-dimensional calculation. So, development of proper analytical solution is one of the aspects of a base work.

2) Analytical solutions of momentum transport for the particular case of flow in reservoirs basins could not be retrieved. So, for the velocity profile, the verification must be pursued by applying the code to cases of enclosed flow cavity for which there are established data available. This is done by modifying the original data, setting inflows and outflows to zero and applying BCs for enclosed cavities.

The model will be implemented by coupling momentum equations in stream function and vorticity formulation to the species transport equation. It is to expect that, once checked on the basis sketched above, it may accurately represent flow and gas concentration profiles in domains depicting hypothetical reservoir basins.

0.6 Closure

This thesis is assumed rewarding as a doctoral study, presenting itself potential of, once attaining its goal, to contribute with:

- 1) Use of vorticity-stream function formulation in 2-D stratified reactive flows;
- 2) Modeling of flows in cavities with a free surface and with momentum and mass efflux;
- 3) Improved way of evaluating wall BCs for the vorticity transport equation;
- 4) Novel downstream BC formulation for parabolic problems;
- 5) Approximation of reservoirs' dynamic processes.

1. SIMULATION OF SPECIES CONCENTRATION DISTRIBUTION IN REACTIVE FLOWS WITH TIME VARYING BOUNDARY CONDITIONS

This thesis is particularly aimed at developing a coherent formulation to be used in 2-D simulations of lengthy reservoirs reactive flows where its depth is comparatively larger than its width, so convective and diffusive effects may be laterally-averaged. The inlet boundary concentration is a pulse, a series of pulses or a continuous periodic function which apply to conditions naturally observed in environmental phenomena, like those related to reservoirs dynamics.

It must be remarked that cyclical, time varying, input imply in outlet conditions not always consistently treated by the usual BCs presented in the literature (OLIVEIRA FILHO et al., 2017). So, an aspect to be approached preliminarily is the study of BCs that can more properly capture the physics of these flows and provide better solutions.

1.1 Outlet Boundary Conditions for the Transport Equation

Usually, three types of BC apply to the species transport equation and for the case of an uncoupled velocity profile \bar{u} :

$$C = \bar{c} \quad \text{on} \quad \Gamma_e \quad (5)$$

$$\frac{\partial C}{\partial \eta} = \bar{q} \quad \text{on} \quad \Gamma_n \quad (6)$$

$$\bar{u}C + \bar{D} \frac{\partial C}{\partial \eta} = \bar{h} \quad \text{on} \quad \Gamma_r \quad (7)$$

where \bar{c} , \bar{q} and \bar{h} may be homogeneous, constant valued or function of time and the greek letter Γ denote the correspondent surface where the BC applies. Equation 5 is usually referred to as Dirichlet or Essential Boundary Condition (EBC), Equation 6, as Neumann or Natural Boundary Condition (NBC) and Equation 7, as Robin or Cauchy Boundary Condition (RBC) and, as consequence, Γ_e is the surface where an EBC applies, Γ_n , where a NBC applies and Γ_r , where a RBC applies.

It must be emphasized that, in the case of time-dependent inlet conditions, special attention must be given to the outlet BC. Since the exit concentration or the species flux is unknown, assuming prescribed values at the outlet is not consistent. It is verified that, to the present, this indeterminacy is treated either by considering that the outlet concentration gradients are zero, which may be physically unrealistic (ZISKIND et al., 2011), or by using Robin type BCs, best suited to represent inlet conditions.

1.2 Literature Review

It is possible to find papers that address the advection–dispersion equation, with or without the reaction term, providing both analytical and numerical solutions. Most of them were written for cases of pollutants discharge, a similar but not identical case as the one of the present concern. However, it is possible to use them as basis for the analysis of concentration profiles in reactive flows.

O’Loughlin and Bowmer (1975), for instance, developed analytical solutions to Equation 4 in 1-D channel flows with decaying species, later extended by Chapman (1979) to

non-uniform steady rivers, both considering only pulse or continuous inlet concentrations and homogeneous NBC for the concentrations at the outlet. Comparison with the results obtained in the experimental works of Vilhena and Leal (1981) for non-reacting pollutants in point source injection shows good agreement with them. Czernuszenko (1987), also working with dispersion of conservative species, proposed a numerical solution for the 2-D advection–diffusion equation, using a conditionally stable finite differences (FD) scheme. But, since the study was restricted to mixing far from the pollution source, leaving convection to the background, the equation was bounded by NBCs, not encompassing unsteady BCs. Piasecki and Katopodes (1997) interested in sensitivity of contaminant concentration profiles to timely changes in its load treated the problem using a FEM scheme, but the unsteady load was a zeroth order production term of the transport equation and the problem was subjected to Dirichlet and Neumann type BCs. Kaschiashvili et al. (2007) provided a consistent model for river reactive flow problems in one, two and three dimensions and used dimension-splitting FD numerical schemes, with unsteady upstream BC and a NBC downstream. But, due to the equilibrium condition at the outlet, consisting of a constant spatial concentration gradient, this BC no longer applies and is modified, sometimes, with the introduction of an additional parameter in order to better reproduce experimental data. The fact supports the remark that time-dependent inlet conditions may imply in difficulties for prescribing values for the outlet conditions. Lee and Seo (2007) used a 2-D finite elements model, based on the Streamline-Upwind Petrov-Galerkin Method (SUPG) together with a Crank-Nicholson FD scheme for the time derivative, but restricted to rivers where the process is diffusion dominated and the downstream BC was a prescribed diffusion flux. Three years later, the same authors employed this same method to accidental mass release in rivers (LEE; SEO, 2010) and, similarly to Piasecki and Katopodes (1997), the accidental mass release was represented by a zeroth order production term of the transport equation which was subjected to Dirichlet inlet BC and Neumann outlet BC, once more not considering unsteady BCs.

As it can be noted, it seems that FEM has a lot of competition from other numerical methods in the simulation of reactive flows, in spite its ability of consistently coping with differential BCs (LOGAN, 2007). This might be explained by the existence of the advective term in the transport equation that makes the system of equations nonsymmetric and prone to numerical oscillations (YU; SINGH, 1995). Several authors addressed the problem by focusing the development of consistent and stable FEM schemes for these flows (YU; SINGH, 1995; GALEÃO et al., 2004; JOHN; SCHMEYER, 2008) but rarely holding their attention on unsteady BCs. The studies of Konzen et al (2007) by which a convective-diffusive-reactive problem formulated through vorticity and stream-function is numerically solved, employing Galerkin FEM (GFEM) together with a Runge-Kutta scheme for the time stepping are also quoted. But, owing to the formulation adopted, the BCs were assumed homogeneous Neumann type and the flow, taking place in a closed cavity, is not subjected to inflows and outflows rates, as in reservoirs.

Therefore, it may be time to focus on the accuracy improvement of numerical schemes that aim the simulation of reactive flows, by considering an unsteady outlet BC that could properly be more consistent with time dependent inlet conditions, as it happens in reservoirs environments.

1.3 Mathematical Formulation

The reaction term in Equation 4 may considerably vary, depending on the process. For simplicity, it was decided to analyze only a first order reaction model for the methane oxidation and the diffusion tensor is assumed constant.

In order to obtain a species transport model that can be verified, at first an uncoupled velocity profile \bar{u} is considered. For simplicity, a linear form, related to the dependence of the diffusion coefficients, is also assumed and the transport equation then becomes:

$$\frac{\partial C}{\partial t} = -\bar{u}_x \frac{\partial C}{\partial x} - \bar{u}_y \frac{\partial C}{\partial y} + D_x \frac{\partial^2 C}{\partial x^2} + D_y \frac{\partial^2 C}{\partial y^2} + kC \quad (8)$$

with initial condition given by:

$$C(x_i, 0) = 0 \quad (9)$$

BCs used at the inlet or upstream are prescribed in one of the two forms below:

$$\left. \begin{aligned} C_{inj}(0,y,t) &= 0, & t &\neq n\tau \\ C_{inj}(0,y,t) &= C_{inj}^*, & t &= n\tau \end{aligned} \right\} \quad (10)$$

in order to represent short injections at arbitrary times $n\tau$, or to represent a periodic injection, it is assumed :

$$C_{inj}(0,y,t) = C_I (1 + \cos m\pi t) \quad (11)$$

where C_I is the mean amplitude of the species concentration at the inlet. In Equations 10-11, the y coordinate dependence is applicable to 2-D flows.

In order to apply a FEM scheme with a Galerkin formulation to solve Equation 8, a weighted residual statement of that equation is elaborated, which reads:

$$\int_{\Omega} \left(\frac{\partial C}{\partial t} + \bar{u}_x \frac{\partial C}{\partial x} + \bar{u}_y \frac{\partial C}{\partial y} - D_x \frac{\partial^2 C}{\partial x^2} - D_y \frac{\partial^2 C}{\partial y^2} - kC \right) w d\Omega = 0 \quad (12)$$

where w is an arbitrary weight function.

By applying the divergence theorem to the third term of Equation 12, and substituting the result in the same equation, the following weak form is obtained:

$$\begin{aligned} \int_{\Omega} \left(w \frac{\partial C}{\partial t} + w \bar{u}_x \cdot \frac{\partial C}{\partial x} + w \bar{u}_y \cdot \frac{\partial C}{\partial y} + D_x \frac{\partial w}{\partial x} \cdot \frac{\partial C}{\partial x} + D_y \frac{\partial w}{\partial y} \cdot \frac{\partial C}{\partial y} - kwC \right) d\Omega = \\ = \int_{\Gamma} w \left(n_x \cdot D_x \frac{\partial C}{\partial x} + n_y \cdot D_y \frac{\partial C}{\partial y} \right) d\Gamma \end{aligned} \quad (13)$$

Having in mind the general shape of the reservoir depicted in Figure 7 and a flow occurring from left to right, one has that $n_x = \vec{n} \cdot \vec{e}_x$, $n_y = \vec{n} \cdot \vec{e}_y$ and that the domain surface is $\Gamma = \Gamma_{in} \cup \Gamma_1 \cup \Gamma_2 \cup \Gamma_{out}$.

Γ_1 and Γ_2 represent upper and lower limit surfaces and have the related fluxes equal to zero. Γ_{in} , by its turn, represents the inlet boundary, subjected to specified, but time-dependent, BCs, as given by Equations 10-11. In this case, the weight functions are zero for Γ_{in} , implying that the surface integral is only evaluated along Γ_{out} . Γ_{out} is the output boundary, comprising only the opening of the dam spillway.

For that outlet surface, it can assume that:

$$\vec{n} = \vec{e}_x \quad (14)$$

and, therefore, the r.h.s. of Equation 13 becomes:

$$\int_{\Gamma_{out}} w \left(D_x \frac{\partial C}{\partial x} \right) d\Gamma_{out} \quad (15)$$

By looking again at Equation 15, it can be verified that the weak formulation boundary term represents the species flux by Fick's Law. Yu and Singh (1995) sustain that this formulation should only be applied to situations where there are exclusively diffusion fluxes at the outlet boundary. But in the problems under consideration, advection effectively occurs at the outlet, and must be taken into account in the BC expression.

In fact, there are cases where gradients normal to the outlet surface are zero, bringing the formulation back onto consistency, even in presence of convection because it eliminates the surface integral. Again considering Equation 15:

$$\left. \frac{\partial C}{\partial x} \right|_{\Gamma_{out}} = 0 \Rightarrow \int_{\Gamma_{out}} w \left(D_x \frac{\partial C}{\partial x} \right) d\Gamma_{out} = 0 \quad (16)$$

One must have in mind that for a developed profile, Equation 16 also implies, taking into account Equation 8, in:

$$\left. \frac{\partial C}{\partial t} \right|_{\Gamma_{out}} = kC \quad (17)$$

It is again emphasized that this condition does not hold when the gradients at the outlet are not zero. It is well known that flow problems involving the transport of chemical species with homogeneous NBC fail to satisfy the conservation law for species concentrations within the domain (GOLZ; DORROH, 2001). In particular, prescribed constant outlet fluxes also do not lead to correct description of time-dependent problems.

So, for the sake of generality another outlet BC must be assumed. For instance, studying momentum transport in such flows, several authors have proposed to prescribe as downstream BC the inviscid momentum equation (BRISTEAU et al., 1987):

$$\frac{\partial \bar{u}}{\partial t} + (\bar{u} \cdot \nabla) \bar{u} + \nabla p = 0 \quad (18)$$

where \bar{u} is the averaged velocity vector and p is the pressure.

Then, it is expected that a similar condition can be applied to the species transport equation. As a strong support for the intention of following the above model and disregard the viscous term of Equation 4 in a new BC, it is pointed out that in the flows under consideration, the species dispersion is mainly due to vertical and transverse velocity gradients, while molecular and turbulent diffusions are generally negligible (LAUNAY et al., 2015).

So, by considering concentration as the dependent variable and inserting the reaction term present in Equation 8:

$$\left(\frac{\partial C}{\partial t} + \bar{u}_i \cdot \frac{\partial C}{\partial x_i} \right) \Big|_{\Gamma_{out}} = kC \Big|_{\Gamma_{out}} \quad (19)$$

where a first order reaction term is adopted to represent methane decay.

Equation 19 is, in fact, a nonhomogeneous material derivative. It depicts a condition, termed Material Derivative Boundary Condition (MDBC) (OLIVEIRA FILHO et al., 2017),

that is constructed with the aim of taking to the outlet surfaces the main phenomena represented by the equation itself, rather than imposing an arbitrary condition at the domain shelf and so, better capture the outlet implications of time-dependent inputs.

In order to profit of MDBC in the formulation, it may be assumed that, at the boundary Γ_{out} , $\bar{u} = \bar{n}\bar{U}$, where $\bar{U} = \sqrt{\bar{u}_x^2 + \bar{u}_y^2}$, what, in general, can match the features of a flow by the spillway of a dam.

Then, Equation 19 can be expressed as:

$$\left(\frac{\partial C}{\partial t} + \bar{U} n_i \frac{\partial C}{\partial x_i} \right) \Big|_{\Gamma_{out}} = kC \Big|_{\Gamma_{out}} \quad (20)$$

where: $n_i = \bar{n} \cdot \bar{e}_i$.

Following, combining equations 13, 15 and 20, it is possible to write:

$$\int_{\Omega} \left(w \frac{\partial C}{\partial t} + w \bar{u}_x \cdot \frac{\partial C}{\partial x} + w \bar{u}_y \cdot \frac{\partial C}{\partial y} + D_x \frac{\partial w}{\partial x} \cdot \frac{\partial C}{\partial x} + D_y \frac{\partial w}{\partial y} \cdot \frac{\partial C}{\partial y} - kwC \right) d\Omega = \int_{\Gamma_{out}} w \frac{D_x}{\bar{U}} \left(kC - \frac{\partial C}{\partial t} \right) d\Gamma_{out} \quad (21)$$

1.4 Numerical Procedure

By using the Galerkin formulation, the concentration profile is approximated by:

$$C_{appr}(x_i, t) = \sum_{j=1}^{NN} C_j(t) S_j(x_i) \quad (22)$$

Substituting this approximation into the weak form given by Equation 21, where, according to the GFEM, the weight functions are the same as the shape functions (ZIENKIEWICZ; TAYLOR, 2000), one has:

$$\sum_{j=1}^{NN} \left\{ \left[\int_{\Omega} S_i S_j d\Omega + \frac{D_x}{\bar{U}} \int_{\Gamma_{out}} S_i S_j d\Gamma_{out} \right] \frac{dC_j}{dt} + \int_{\Omega} S_i \left(\bar{u}_x \frac{\partial S_j}{\partial x} + \bar{u}_y \frac{\partial S_j}{\partial y} \right) + \left(D_x \frac{\partial S_i}{\partial x} \frac{\partial S_j}{\partial x} + D_y \frac{\partial S_i}{\partial y} \frac{\partial S_j}{\partial y} \right) \right] d\Omega C_j - k \left[\int_{\Omega} S_i S_j d\Omega + \frac{D_x}{\bar{U}} \int_{\Gamma_{out}} S_i S_j d\Gamma_{out} \right] C_j \right\} = 0 \quad (23)$$

where the boundary integral (r.h.s of Equation 21) was approximated through:

$$\sum_{j=1}^{NN} \left[\frac{D_x}{\bar{U}} \left(\int_{\Gamma_{out}} S_i S_j d\Gamma_{out} \right) \left(kC_j - \frac{dC_j}{dt} \right) \right] \quad (24)$$

Equation 23 encompasses a stiffness matrix and a modified mass matrix which is related to the concentration time derivative $\left\{ \dot{C} \right\}$ and the reaction term. It can be put in matrix form as:

$$[M_1] \left\{ \dot{C} \right\} + [K] \{C\} - k[M_1] \{C\} = 0 \quad (25)$$

where, M_1 and K are, respectively, the modified mass and stiffness matrices.

In order to solve Equation 25, it is employed a numerical scheme, using the Crank-Nicholson Method (LEWIS et al., 2005), which reads:

$$\{C_{t+1}\} = \left([M_1] + \frac{\Delta t}{2} (K - k[M_1]) \right)^{-1} \left([M_1] - \frac{\Delta t}{2} (K - k[M_1]) \right) \{C_t\} \quad (26)$$

It must be observed that it is also possible to look for another solution without modifying the original mass matrix, as suggested above. In this case, the use of the Crank-Nicholson scheme on GFEM approximation of Equation 13, implies in:

$$\{C_{t+1}\} = \left([M] + \frac{\Delta t}{2} [K_1] \right)^{-1} \left[\left([M] - \frac{\Delta t}{2} [K_1] \right) C_t + \frac{\Delta t}{2} (\{B\}_t + \{B\}_{t+1}) \right] \quad (27)$$

where $\{B\}_t$ and $\{B\}_{t+1}$ are the boundary terms arising from the line integral approximation on the r.h.s of Equation 13 at times t and $t+1$, $[M]$ is $\sum_{j=1}^{NN} \int_{\Omega} S_i S_j d\Omega$ and $[K_1]$ is a modified stiffness matrix, now including the decay term, last on the left term of Equation 21, or:

$$\sum_{j=1}^{NN} \left\{ \int_{\Omega} \left[S_i \left(\bar{u}_x \frac{\partial S_j}{\partial x} + \bar{u}_y \frac{\partial S_j}{\partial y} \right) + \left(D_x \frac{\partial S_i}{\partial x} \frac{\partial S_j}{\partial x} + D_y \frac{\partial S_i}{\partial y} \frac{\partial S_j}{\partial y} - k S_i S_j \right) \right] d\Omega \right\} \quad (28)$$

In this case, the boundary vectors ($\{B\}_t$ and $\{B\}_{t+1}$) must be evaluated using Equation 24. Being dependent on the concentration and its time derivative in past and present time steps, these vectors must be continuously updated, making the numerical scheme for solving Equation 26 simpler than the one required for solving Equation 27. Thus, the first scheme was adopted.

1.5 Analytical Solutions to the CDRE

This class of problems has already motivated many studies pursuing analytical solutions of convection-diffusion-reaction equations—subjected to time-dependent BCs, like the ones from van Genuchten and Alves (1982), Logan and Zlotnik (1995), Logan (1996), Aral and Liao (1996), Golz and Dorroh (2001), Chen and Liu (2011) and Pérez Guerrero et al. (2013). These studies are mostly restricted to 1-D cases when reservoirs, usually with large dimensions, ask for multidimensional calculations. However, it is interesting to consider some of these solutions for purposes of model verification.

In the simplest case of 1-D flow, analytical solutions for continuous and pulse mass injection, are, respectively (O'LOUGHLIN; BOWMER, 1975; CHAPMAN, 1979):

$$\frac{C(x,t)}{C_{inj}} = \frac{1}{2} \exp\left(\frac{-kx}{\bar{u}_x}\right) \operatorname{erfc}\left[\frac{x - \bar{u}_x t(1 + H_x)}{\sqrt{4D_x t}}\right] \quad (29)$$

and:

$$C(x,t) = \frac{M_{inj}}{\sqrt{4\pi D_x t}} \exp\left[-kt - \frac{(x - \bar{u}_x t)^2}{4D_x t}\right] \quad (30)$$

where $H_x = \frac{2kD_x}{\bar{u}_x^2}$ and M_{inj} is the total mass injected per unit area.

And for a 2-D case with pulse injection where there is a transversal diffusion D_y and zero lateral component of velocity (VILHENA; SEFIDVASH, 1985):

$$C(x,y,t) = \frac{M_{inj}}{4\pi t \sqrt{D_x D_y}} \exp\left\{-\left[kt + \frac{(x - \bar{u}_x t)^2}{4D_x t} + \frac{y^2}{4D_y t}\right]\right\} \quad (31)$$

Furthermore, it is not necessary to assume that the inlet BCs given by Equations 10-11 occur independently in order to obtain a more generic solution. If it is considered that they are time dependent, isolated or combined they have a Fourier representation, under a time periodic form as $f(t)$. In this way, an one-dimensional analytical solution may be obtained.

By following the work of Logan and Zlotnik (1996), it is possible to establish that Equation 8 clearly admits a solution of the form:

$$C(x,t) = e^{\hat{\alpha}x + \hat{\beta}t} \quad (32)$$

where $\hat{\alpha}$ and $\hat{\beta}$ are complex valued, thus:

$$\hat{\alpha} = \alpha_R + i\alpha_I \quad \text{and} \quad \hat{\beta} = \beta_R + i\beta_I \quad (33)$$

Then, substituting Equations 32-33 in the 1-D form of Equation 8, one obtains:

$$\hat{\beta} = k - \bar{u}_x \hat{\alpha} + D_x \hat{\alpha}^2 \quad (34)$$

Once the periodic BC forces the inlet concentration at a fixed value, $\beta_R = 0$ and the solution may be expressed as:

$$C(x,t) = \mathbf{R}\left[e^{(\alpha_R + i\alpha_I)x + i\beta_I t}\right] \quad (35)$$

where \mathbf{R} means the real part of Equation 35 and:

$$\alpha_I = \pm \sqrt{\alpha_R^2 - \frac{\bar{u}_x}{D_x} \alpha_R - \frac{k}{\bar{u}_x}} \quad \text{and} \quad \beta_I = \pm \sqrt{\alpha_R^2 - \frac{\bar{u}_x}{D_x} \alpha_R - \frac{k}{\bar{u}_x}} (2D\alpha_R - \bar{u}_x) \quad (36)$$

Also, considering that the concentration at $x = 0$ cannot take negative values, it is necessary to add a constant forcing, such that this restriction is satisfied, and Equation 35 becomes:

$$C(x,t) = C_o + \mathbf{R}\left[e^{(\alpha_R + i\alpha_I)x + i\beta_I t}\right] \quad (37)$$

For this constant forcing, obviously $\beta_R = \beta_I = 0$ and therefore, with the use of Equation 36:

$$\hat{\alpha}_o = -\frac{\bar{u}_x}{2D_x} \pm \sqrt{\frac{\bar{u}_x^2}{4D_x} - \frac{k}{D_x}} \quad (38)$$

what implies in:

$$C_o = \mathbf{R} \left[e^{(\hat{\alpha}_o)x} \right] \quad (39)$$

Thus, given k , \bar{u}_x and D_x , as well as an arbitrary α_R , the analytical solution may be constructed, employing Equations 36-39.

As conditions applicable to cyclic environmental conditions found in the reservoirs under consideration may be represented by continuous periodic functions, a 2-D analytic solution to the CDRE may be constructed in order to aid verification of the two-dimensional model.

In this case, one may consider as ansatz:

$$C(x, y, t) = e^{\hat{\alpha}_x x + \hat{\alpha}_y y + \hat{\beta} t} \quad (40)$$

Once more, observing that $\hat{\alpha}_i$ and $\hat{\beta}$ are complex valued:

$$\hat{\alpha}_x = \alpha_{xR} + i\alpha_{xI}, \quad \hat{\alpha}_y = \alpha_{yR} + i\alpha_{yI} \text{ and } \hat{\beta} = \beta_R + i\beta_I \quad (41)$$

By substituting the relations of Equation 40 in the ansatz (Equation 39), one obtains:

$$\hat{\beta} = k - \bar{u}_x \hat{\alpha}_x - \bar{u}_y \hat{\alpha}_y + D_x \hat{\alpha}_x^2 + D_y \hat{\alpha}_y^2 \quad (42)$$

Similarly to the one-dimensional case, taking real and imaginary parts of Equation 42:

$$\beta_R = k - \bar{u}_x \alpha_{xR} - \bar{u}_y \alpha_{yR} + D_x (\alpha_{xR}^2 - \alpha_{xI}^2) + D_y (\alpha_{yR}^2 - \alpha_{yI}^2) \quad (43)$$

$$\text{and: } \beta_I = -\bar{u}_x \alpha_{xI} - \bar{u}_y \alpha_{yI} + 2D_x \alpha_{xR} \alpha_{xI} + 2D_y \alpha_{yR} \alpha_{yI} \quad (44)$$

Considering periodicity in the y direction, hence β_R and α_{yR} are set to zero, in order to obtain bounded solutions, while α_{yI} is an arbitrarily prescribed constant, in order to properly represent oscillations in the y coordinate.

Supposing an isotropic diffusion tensor, in order to simplify the solution, one obtains, after inserting the above conditions in Equation 43 and substituting in Equation 43:

$$\alpha_{xI} = \pm \sqrt{\alpha_{xR}^2 - \alpha_{xI}^2 - \frac{\bar{u}_x}{D} \alpha_{xR} + \frac{k}{D}} \quad (45)$$

which, upon substitution in Equation 43, yields:

$$\beta_I = \pm \sqrt{\alpha_{xR}^2 - \alpha_{xI}^2 - \frac{\bar{u}_x}{D} \alpha_{xR} + \frac{k}{D}} (2D\alpha_{xR} - \bar{u}_x) - \bar{u}_y \alpha_{yI} \quad (46)$$

and the solution can be expressed as:

$$C(x, t) = C_o + \mathbf{R} \left[e^{(\alpha_{xR} + i\alpha_{xI})x + i\alpha_{yI}y + i\beta_I t} \right] \quad (47)$$

Also, to assure the nonnegative restriction for the concentration profile, $\beta_I = 0$, which supplies the constant forcing:

$$C_o = e^{\hat{\alpha}_x x + i\alpha_{yI}y} \quad (48)$$

where α_{yI} is arbitrarily prescribed and:

$$\hat{\alpha}_x = \frac{\bar{u}_x}{2D} \pm \sqrt{\frac{\bar{u}_x^2}{4D^2} - \left(\frac{k - \bar{u}_y i \alpha_{yI} - D \alpha_{yI}^2}{D} \right)} \quad (49)$$

Although referring to the linear species transport equation, the solutions may work as a basis for the model verification. In the same way as the 1-D case, the solution, employing Equations 45 to 49 may be constructed. Further insight on the solution development held from Equation 32 on can be found in Annex A of this thesis.

1.6 Code, Methods and Verification

The numerical procedure described before was programmed in MATLAB, as mentioned before, using GFEM. The integrals in Equation 23 were evaluated by the GQ. The solution domain was discretized in regular triangular or quadrangular element meshes by routines within the program, depending on the case run. The program is also capable of performing GQ calculations in diversified number of interval points. Linear shape functions were used throughout, so precision of the scheme was controlled by properly refining the mesh.

It is well known that simple GFEM presents numerical oscillations and instabilities in problems where advection is important. So, more elaborated FEM schemes would be required to solve problems with small diffusion coefficients. However, considering that the role of the unsteady BC along with the outlet BC represented by a material derivative were the main aspects to be investigated, this method was employed with restrictions. Aware that some of the major factors causing these issues are improper choice of a time step size and also of element size and shape (YU; SINGH, 1995), it was adopted, as a basis for the time step and element size control, respectively, (CHAPRA; CANALE, 2010):

$$\Delta t_i \leq \frac{(\Delta x_i)^2}{2D_{x_i} + k \cdot (\Delta x_i)^2} \quad \text{and} \quad \Delta x_i \leq \frac{2D_{x_i}}{\bar{u}_i} \quad (50)$$

In order to test the code with the analytical solutions given by Equations 29-31, the inlet BCs to be applied at $x=0$ must carry on the initial shape of the defined concentration, as suggested by Yu and Li (1998). This implies in:

a) for Equation 29:

$$C_o(0, t) = \frac{C_{inj}}{2} \left\{ \operatorname{erfc} \left[\frac{-\bar{u}_x t (1 + H_x)}{\sqrt{4D_x t}} \right] \right\} \quad (51)$$

b) for equation 30:

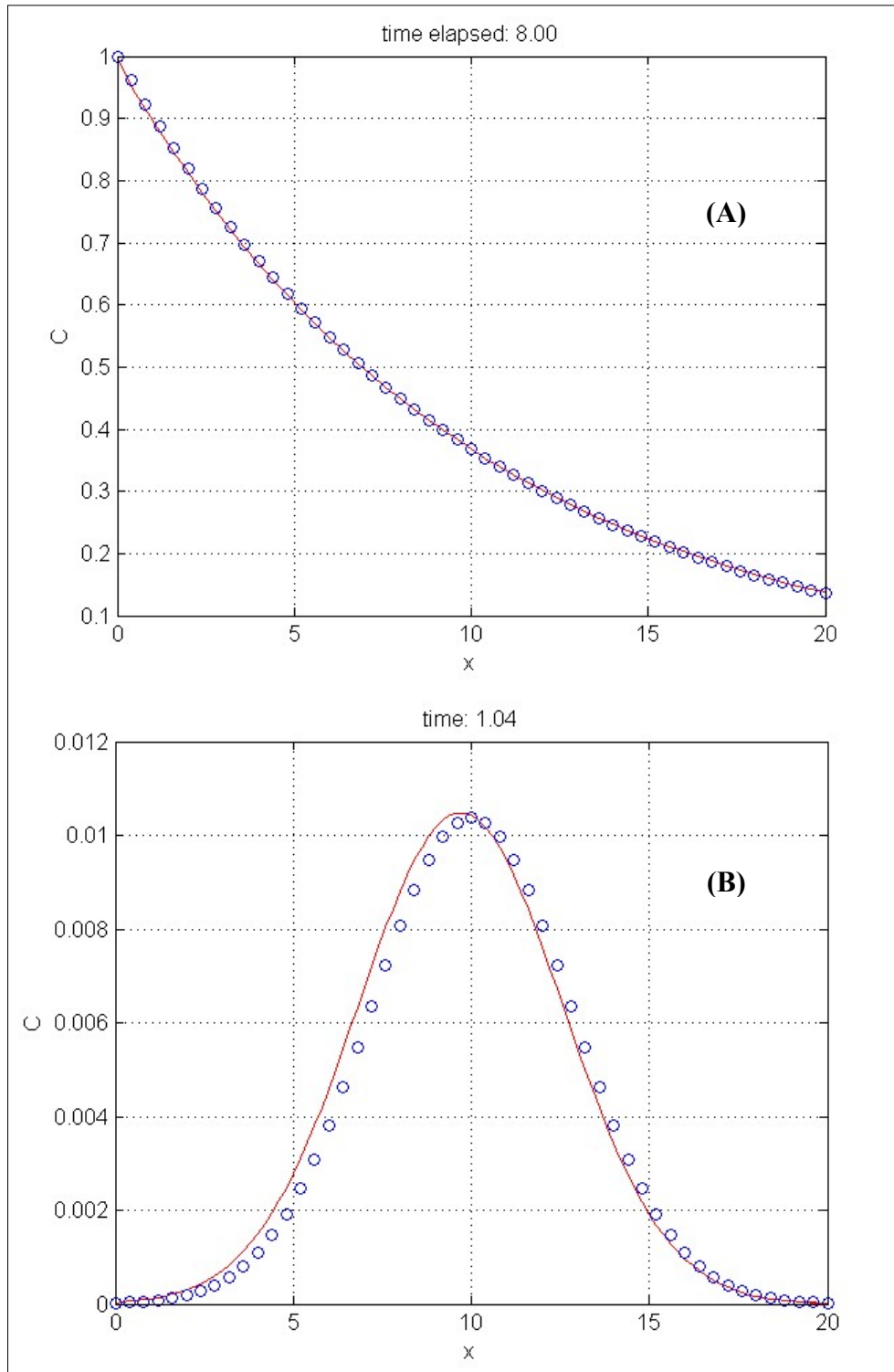
$$C_o(0, t) = \frac{M_{inj}}{\sqrt{4\pi D_x t}} \exp \left[-kt - \frac{(-\bar{u}_x t)^2}{4D_x t} \right] \quad (52)$$

c) for equation 31:

$$C_o(0, y, t) = \frac{M_{inj}}{4\pi t \sqrt{D_x D_y}} \exp \left[-kt - \frac{(-\bar{u}_x t)^2}{4D_x t} - \frac{y^2}{4D_y t} \right] \quad (53)$$

Having that in mind, for constant and pulse injection cases the concentration profiles plotted in the figures below are obtained.

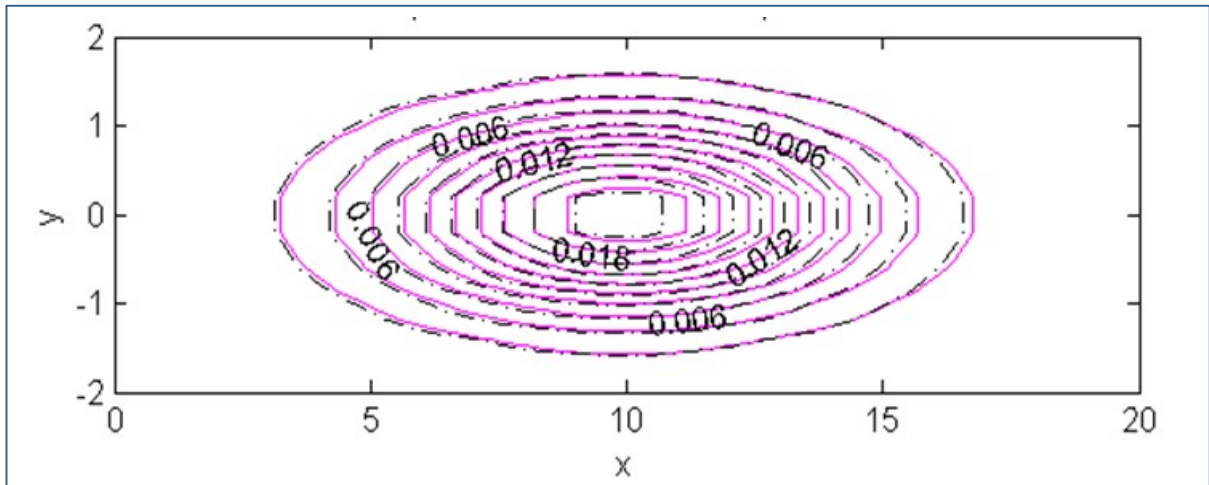
Figure 9 – 1-D analytical and numerical solutions of equations 29-30.



Tags: (A) – Equation 29, $Pe = 200$; (B) – Equation 30, $Pe = 50$;

ooo – Analytical Solution; — Numerical Solution.

Figure 10 – 2-D analytical and numerical solutions of equation 31 (1250 elements mesh FEM; GQ 9 points; Pe=50; time elapsed = 1.20)

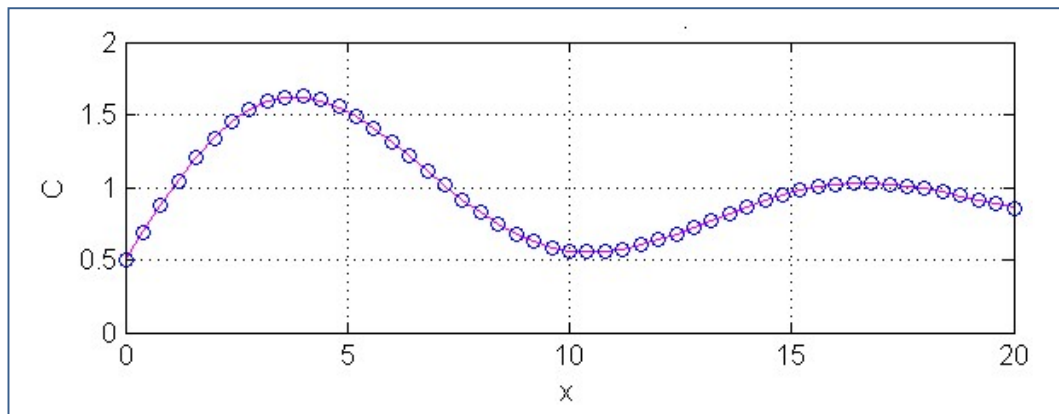


Tags: — Analytical Solution; - - - - Numerical Solution.

In the Figures 9-10, being the characteristic dimension depicted by the horizontal axis ($x = 20$), conditions for $Pe = 50$ are: $\bar{u}_x = 10$, $D_x = 4.0$ and $k = 1.0$ and for $Pe = 200$ are: $\bar{u}_x = 10$, $D_x = 1.0$ and $k = 1.0$, resulting in the same Damköhler Number (2.0) for all cases. For 2-D test, case of Equation 30, which admits a lateral component of diffusion, D_y was set equal to 0.2. The 1-D tests were conducted setting the y coordinate components to zero and the 2-D tests assumed that y represents the reservoir width, instead of its depth, as it will be employed in the reservoir simulation.

The numerical solution for the periodic inlet BC (Equation 11) may be compared with the 1-D analytical solution constructed from Equations 35-38. Figure 11 shows the outcome for $Pe = 100$, where $\bar{u}_x = 5.0$, $D_x = 1.0$ and $k = 0.1$, implying in $Da = 0.4$. Again, the 1-D numerical plot is obtained by setting the y coordinate components of the code to zero.

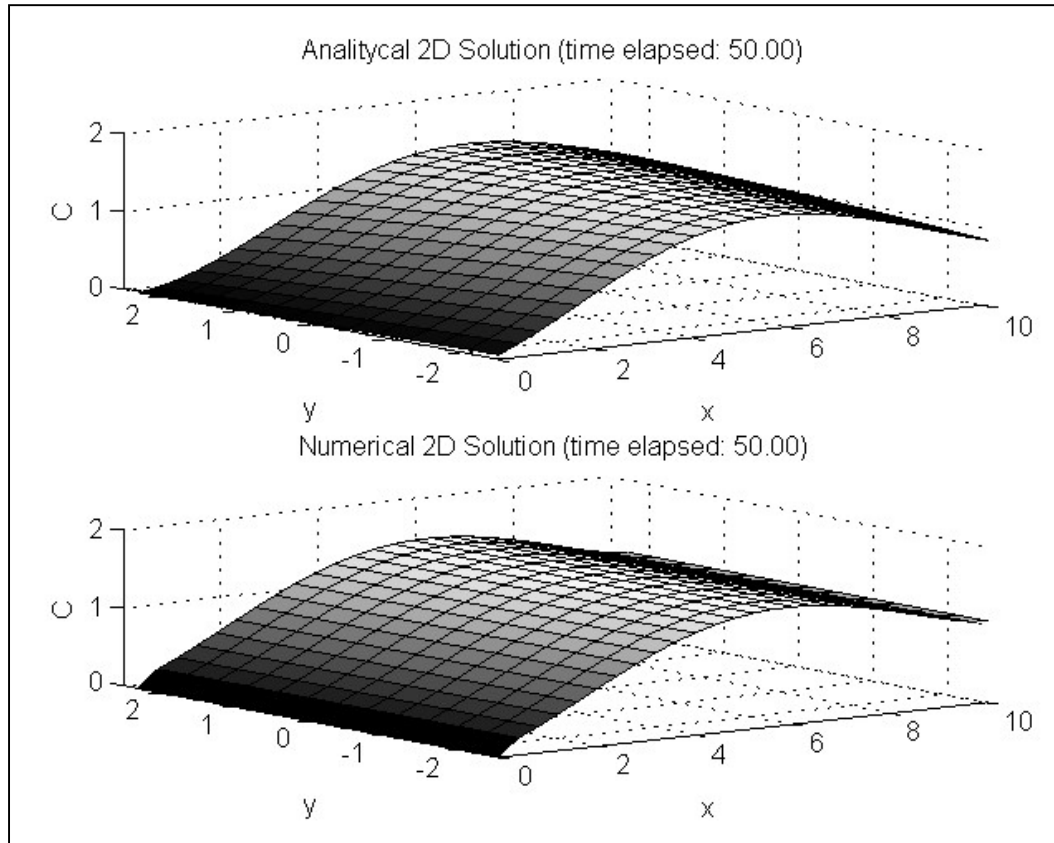
Figure 11 – 1-D analytical and numerical solutions with periodic inlet BC (1250 elements mesh FEM; GQ 9 points; Pe=100; time elapsed = 10.0)



Tags: ooo – Analytical Solution; — Numerical Solution.

2-D numerical solution for the periodic inlet, by its turn is compared to the developed analytical solution. The outcome shown in the following figure is a frame obtained for an elapsed time of 50.0 in an hypothetical basin such as length (x) = 10, width (y) = 5, $k = 0.01$, $\bar{u}_x = 2.0$, $\bar{u}_y = 0.2$ and $D = 1.0$. α_{xR} and α_{yI} were arbitrarily set to -0.1

Figure 12 – 2-D analytical and numerical solutions with periodic inlet BC.



Other results were obtained, varying elapsed times, and the error was evaluated through Root Mean Square Deviation (RMSD), or:

$$\text{RMSD} = \sqrt{\frac{\sum_{i=1}^{nd} (C_i - C_i^a)^2}{nd}} \quad (54)$$

where C_i^a is the analytical solution at node i for a given total number of nodes nd . Table 2, below, shows said RMSD evaluations.

Table 2 – Figure 12 correspondent RMSD.

t	RMSD
30.0	0.0589
50.0	0.0547
70.0	0.0691

In order to obtain these plots, numerical calculations were performed respecting the stability restrictions posed by Equations 50. The plots show good agreement between analytical and numerical solutions even for high Péclet Numbers.

It is possible to observe a better agreement between analytical and numerical solutions for the continuous injection case, as shown in plot A of Figure 9. The plot B of Figure 9 and the plot of Figure 10 show that the numerical curves are slightly delayed compared to the exact solutions. This delay results from the fact that the discrete time integration cannot completely follow the instant moment of mass release (LEE; SEO, 2010). RMSD calculations shown in Figure 12 reveal acceptable deviations from the exact solution for the two-dimensional case (Table 2).

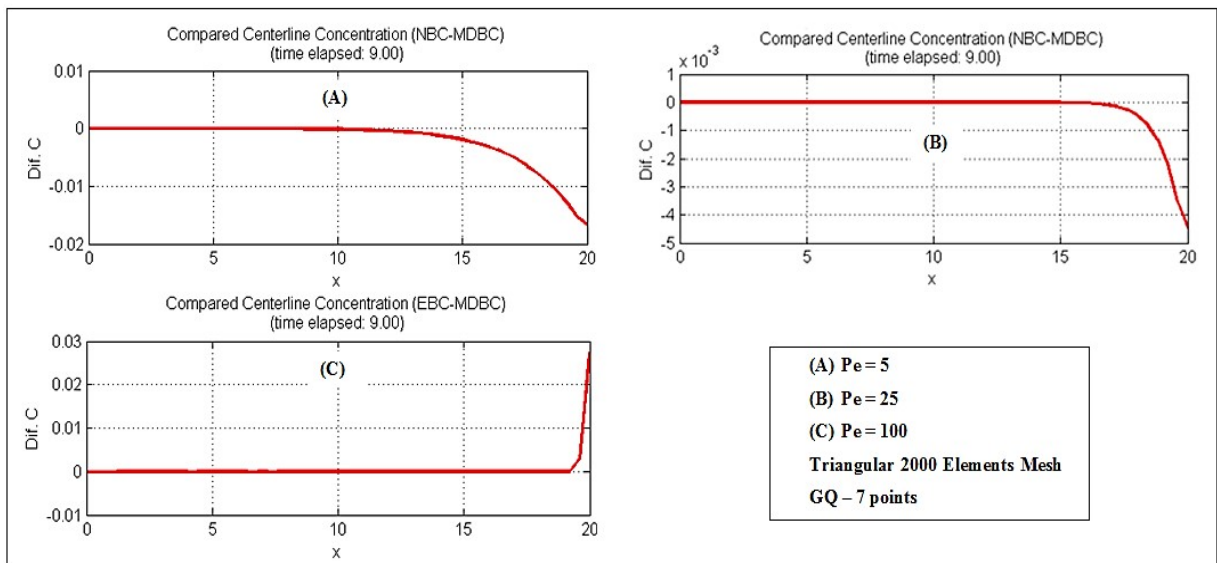
Thus, it can be concluded that the code has been verified and is able to present reliable simulations of concentration profiles in reactive flows.

1.7 Use of MDBC compared to EBC and NBC for finite domains

The analytical solutions which were used to verify the code assume Neumann's outlet BCs at semi-infinite domains which is a plausible condition to reach consistent solutions naturally applicable to very long domains. Otherwise, solutions for finite domains that accept EBC or NBC are subjected to criticism (ZISKIND, 2011). So, in order to verify the validity of using MDBC in these domains, 1-D solutions of Equation 8 subjected to a time periodic inlet that adopt EBC, NBC or MDBC were compared.

Figure 13 compares simulated concentration profiles for sorted conditions, such as $Pe = 5$ ($\bar{u}_x = 1.0$; $D_x = 4.0$; $k = 0.1$), $Pe = 25$ ($\bar{u}_x = 5.0$; $D_x = 4.0$; $k = 0.1$) and $Pe = 100$ ($\bar{u}_x = 5.0$; $D_x = 1.0$; $k = 0.1$). In order to obtain the plots, a 1-D form of Equation 8 subjected to a time periodic inlet BC (Equation 11) is solved, changing the outlet BC type. First, an EBC arbitrarily set to a given constant value is employed, then, a homogeneous NBC and last, the proposed MDBC. Then, the concentrations differences (Dif C) along coordinate x were plotted.

Figure 13 – 1-D concentration profile differences – numerical solutions (Outlet BC: 0.5; Outlet NBC: Equation 16; Outlet MDBC: Equation 20).



As it can be seen, profiles obtained when the adopted outlet condition is either EBC or the homogeneous NBC, compared to those obtained by the adoption of the MDBC, concentrate larger differences around the exit.

Thus, in order to check which is the best suited BC for the case in study, concentrations 1-D profiles for various flow and reaction parameters were numerically evaluated. The results were compared to the analytical solution applying the RMSD (Equation 54) around the domain exit. This implies that, in this case, nd is restricted to the total number of nodes at the outlet region.

Table 3 – RMSD between 1-D analytical and numerical solutions.

Pe = 100		RMSD			
Δx	Δt	Da	An. - EBC	An. - NBC	An. - MDBC
0.2	0.02	0.1	0.8193	0.0315	0.0226
		1.0	0.2640	0.1839	0.1744
		2.0	0.0745	0.0044	0.0022
Pe = 50		RMSD			
0.2	0.005	0.1	0.8628	0.0098	0.0041
	0.05	1.0	0.4982	0.0106	0.0032
		2.0	0.1312	0.0809	0.0798
Pe = 25		RMSD			
0.2	0.02	0.1	0.8846	0.0777	0.0537
0.4	0.01	1.0	0.4010	0.0676	0.0679
0.2	0.02	2.0	0.1476	0.0387	0.0259
Pe = 5		RMSD			
0.2	0.05	0.1	0.6155	0.0275	0.0191
	0.2	1.0	0.5672	0.0071	0.0072
	0.1	2.0	0.0880	0.0178	0.0034

(Outlet EBC = 0.0; Outlet NBC: Equation 16; Outlet MDBC: Equation 20)

It is observed that the numerical solutions with outlet EBC provide the poorest approximations in all Péclet and Damköhler Numbers considered and that MDBC solutions result in better approximations than NBC in almost all cases. This is possibly due to the fact that MDBC better captures specific features of the flow because it encompasses, in its formulation, physical effects of the problem which are not present in the usual types of BCs.

Results on Table 3 also point at examples where the advantages of using MDBC instead of homogeneous NBC are not clear. Such situations arise from particular flow conditions that imply in very small concentration gradients at the outlet, as consequence of Péclet and Damköhler Numbers combinations. These cases approach patterns that can be treated conveniently by the homogeneous NBC and so, when outcomes obtained both with the use of NBC and MDBC are compared, it is verified analogous deviation from the analytical solution. However, these are special cases of the problem and the use of the MDBC for more general formulations is established.

1.8 Closure

In transient reactive flow problems subjected to unsteady BC the main issue is to achieve physical coherence in constructing the model to be solved. Some analytical solutions of this class of problems are found in the literature which, though being parabolic, usually assume the outlet BC in the form of a constant concentration or of a given concentration gradient.

As indicated by Piasecki and Katopodes (1997), the simulations confirmed that oscillatory inlet conditions result in time-dependent concentrations at the outlet, that cannot be

accounted for by EBCs and NBCs. Also, NBCs may not represent the total equilibrium flux at the outlet (YU; SINGH, 1995), leading to physically incomplete models that could perform imprecise profile estimation.

A new procedure was then proposed, by which a material derivative is considered as the outlet BC. Results show that these BCs provide a better picture of the process, once they provide automatic updating of the outlet equilibrium concentration.

This contribution will be employed in the formulation of Equation 4 of the system encompassed by Equations 2 to 4 and generalized in the formulations of Equations 2 and 3. It is also necessary to remark that Equation 13, although inheriting the linear form from Equation 8, can be applied to nonlinear problems through FEM. This is because in the construction of the approximate solution, the coefficients may be considered locally constants, being evaluated along the mesh, depending on the element coordinates. See, for instance, function `calcSElem(e)` in Appendix B.

Further aspects of this section can be found in Annex B.